V/STOL Propulsion Control Technology

Harold Brown*
General Electric Company, Cincinnati, Ohio

This paper represents the results of a two-year study of propulsion control requirements, design concepts and procedures, and control designs for a supersonic V/STOL propulsion system. A variable cycle engine with remote augmented lift system was used as a baseline for establishing typical operating requirements and control concepts. Multivariable control design techniques were used to establish regulator gain schedules and control concepts. A nonlinear engine model was developed for control development and evaluation and as a precursor to a real-time simulation capability. This paper presents the principal results of this study and provides recommendations for subsequent work needed.

Nomenclature

A8R	= regulator output correction on A8
A80	= RFCV flow area
A88R	= regulator output correction on A88
A,B,C,D	= state-space model matrices
a,b,c,d	= elements of A,B,C,D matrices
AEBG	= General Electric Aircraft Engine Business Group
a	= regulator proportional gain coefficient
b	= regulator integral gain coefficient
C	= measurable variable vector
FG	= total gross thrust
FG8	= ADEN gross thrust
FI	= flight idle
FICA	= failure indication and corrective action
K	= elements of K matrix
K matrix	= engine controller matrix
LEM	= linear engine model
M	= variable geometry (manipulated variable) vector
M93	= fan discharge Mach number
N2	= low-pressure rotor speed
N25	= high-pressure rotor speed
P	= performance parameter vector
P6	= primary augmentor inlet pressure
PCN2	= percent low-pressure rotor speed
PS3	= compressor discharge static pressure
Q	= engine tolerance and decrement vector
Q matrix	= engine dynamic response matrix
RDL	= RALS deflection angle (longitudinal)
RDT	= RALS deflection angle (transverse)
S	= Laplace transform
SM2	= front-block fan stall margin
SM25	= compressor stall margin
STP22	= rear-block fan stator position angle
T41	= high-pressure turbine inlet temperature
T5	= low-pressure turbine discharge temperature
U	= control variable vector
X	= state variable vector
$\dot{X}$	= state variable rate-of-change vector
Y	= output vector

Presented as Paper 81-2634 at the AIAA/NASA Ames VSTOL Conference, Palo Alto, Calif., Dec. 7-9, 1981; submitted Dec. 17, 1981; revision received March 29, 1983.

*Manager, Aerothermo Systems, Aircraft Engine Business Group.

Introduction

THE V/STOL propulsion control system can be expected to be one of the more critical elements of an operational supersonic V/STOL aircraft. The propulsion system must be effectively integrated with the aircraft flight control system during the vertical and low flight speed operating regime. The propulsion control must transition the propulsion system between its vertical and horizontal operating configurations. It must also provide traditional propulsion control capabilities in the conventional flight regime. A study has been conducted for the development of supersonic V/STOL propulsion control requirements, design concepts and procedures, and a typical V/STOL propulsion control design. The overall objective of the study was to produce a mathematical model of a typical supersonic V/STOL propulsion and control system which could be used in subsequent programs to achieve a real-time piloted simulation capability for concept verification and evaluation.

Discussion

Baseline Engine

A baseline engine concept was selected in order to provide a source of propulsion control requirements and operating characteristics which could be used as the basis for the control design concepts and the mathematical model of a typical system. Figure 1 illustrates the variable cycle engine (VCE) with remote augmented lift system (RALS) that was selected as the baseline.[1] The basic engine includes an oversized two-stage fan, a core-driven third stage, and a variable area low-pressure turbine (VALPT). It utilizes a rear variable area bypass injector (VABI) to regulate the flow to the remote system.[2] The cold side of the VABI is closed during vertical operations and all bypass duct flow is directed to the remote augmentor and nozzle. Nominal primary and remote augmentor operation produces 45% of total engine thrust in the remote nozzle and the remaining 55% in the augmented deflected exhaust nozzle (ADEN)[3] used for the primary nozzle. Primary and remote augmentor fuel-flow modulation produces a ±12% thrust modulation capability in each nozzle, which is used in conjunction with thrust vectoring for height, pitch, and yaw control during vertical and low-speed flight operations. Roll control is provided by compressor bleed air which is ducted to wing-tip puffer jets.

Horizontal thrust is obtained for transition to conventional flight by rotating the ADEN toward the horizontal position, by opening the cold side of the VABI to reduce the airflow to the remote system, and by modulating the RALS fuel flow to maintain pitch balance. The RALS system is completely shut down during conventional horizontal flight and all bypass duct flow passes through the VABI and is exhausted along with the primary core flow through the ADEN.

Steady-State Operating Characteristics

Figure 2 shows typical VCE-RALS steady-state thrust capabilities at a flight condition in the vertical or low-flight speed operating regimes. It contains lines of total thrust and thrust split (remote thrust/primary thrust) plotted against the primary ADEN thrust and the RALS thrust. It addresses the three primary modes of thrust modulation which must be provided by the V/STOL propulsion control system.

Total engine thrust is set by the engine control that regulates primary fuel flow, engine rotor speeds, and internal engine geometry. The engine control uses a nominal VABI area schedule to set the nominal thrust split between the primary and remote nozzles and nominal augmentor fuel schedules to set the nominal operating point at the center of the small operating box. Changes in total thrust demand are accommodated by changes in primary engine fuel flow and rotor speeds, which slide the operating box to the left along a constant thrust split line.

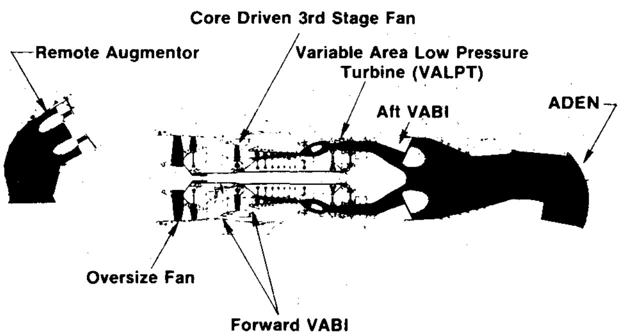

Fig. 1 VCE/RALS baseline engine.

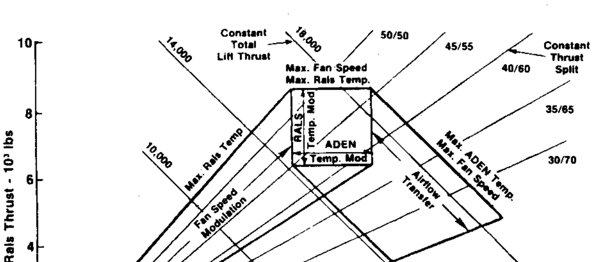

Fig. 2 RALS thrust modulation in VTOL mode.

Table 1 Transition operating points

Mode	Operating point	RALS flow rate, %	Thrust ratio, %FG89/FG	TVA, deg
VTH	Takeoff	100	45	90
	Start transition	99	44	77
	Activate RFCV	80	32	36
	Midtransition	50	13	11
	Minimum RALS	30	3	2
	Maximum horizontal	0	0	0
HTV	Flight idle descent	0	0	0
	Initiate RALS flow	30	5	4
	Minimum augmentation	60	14	12
	Midtransition	80	35	41
	Landing	100	45	90

Thrust split is set by modulating the VABI area relative to its nominal schedule in order to change the amount of bypass duct air to the remote system. This is accomplished by the thrust vector control system. Primary and remote augmentor fuel flows are adjusted with the remote system flow to maintain nominal augmentation levels in the primary and remote systems. This process slides the operating box downward along a constant total thrust line.

The individual primary and remote thrust levels are varied by the flight control system in response to demands for height, pitch, and yaw control corrections. This is accomplished by modulating the primary and remote augmentor fuel flows relative to their nominal schedules and can translate the operating point from the center of the operating box to any point within its boundaries. The baseline engine has been configured for a ±12% thrust modulation capability in each augmentor at all operating conditions. The propulsion system must also respond to ADEN and RALS nozzle deflection commands, which are expected to be transmitted directly from the aircraft flight control system.

Transition from the vertical flight regime to horizontal flight is accomplished by transferring bypass flow from the remote system to the VABI and by rotating the increased ADEN thrust vector toward the axial direction to accelerate the aircraft. The remote nozzle thrust vector is held in the vertical direction, the remote augmentor fuel flow is reduced to maintain the nominal augmentation rate, and the ADEN thrust vector angle (TVA) is decreased to maintain a zero propulsive pitching moment about the aircraft. Figure 3 shows the resulting variations in ADEN thrust, RALS thrust, and ADEN thrust vector angle for this mode of operation at sea level static conditions. The remote augmentor must be shut down when the remote flow Mach number can no longer support stable combustion and this regime is shown by the cross-hatched region of the curve. Flight control inputs may modulate the RALS augmentation rate relative to a nominal transition schedule if required. The vertical to horizontal transition (VTH) boundary represents maximum transition thrust requirements and is based on a transition from vertical takeoff to horizontal acceleration for a maximum gross weight aircraft. The VTH boundary represents minimum thrust requirements and is based on a transition from horizontal idle descent to vertical landing for a minimum gross weight aircraft. A full envelope control system must operate the engine over the total region indicated in Fig. 3.

Specific steady-state operating points were selected along the VTH and horizontal to vertical transition (HTV) operating boundaries and are summarized in Table 1. RALS flow rate (% of total bypass flow), RALS thrust ratio (% of total thrust), and the corresponding ADEN thrust vector angle is indicated for each point. These points represent discrete actions by the propulsion system and were used for establishing steady-state operating requirements and

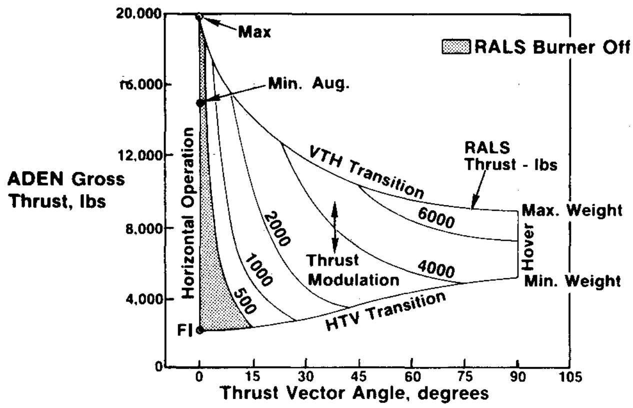

Fig. 3 Thrust modulation during transition.

schedules, for control mode studies, regulator design studies, and for the component regression modeling process.

Control Mode Study

The baseline engine control system is responsible for setting the following variables during conventional horizontal flight: rear block fan stator position, compressor stator position, primary fuel flow, low-pressure turbine diaphragm area, rear VABI area, primary augmentor fuel flow, and exhaust nozzle area.

The following additional variables must also be set during vertical and transitional operations: remote flow control valve, remote augmentor fuel flow, remote nozzle area, remote longitudinal deflection angle, remote transverse deflection angle, and ADEN longitudinal deflection angle. The control mode study is used to determine which variables should be controlled closed-loop and which engine-measurable variables should be used in the closed-loop control process.

The mode study is based on a steady-state linear model, which is derived from a nonlinear model of the engine, and a series of variational models derived from prior engine operating experience. The linear engine model represents a matrix of partial derivatives which provide the changes in each engine performance parameter and measurable variable due to changes in each of the above engine-manipulated variables. Variables which do not effect internal engine operation, such as the three nozzle deflection angles, are omitted from the process. An engine component tolerance model is used to provide 2-σ variations in the engine component performance parameters (component efficiencies, flow rates, pressure drops, and parasitic flows). The engine tolerances represent expected variations due to new engine manufacturing and assembly tolerances. A control tolerance model is used to provide corresponding 2-σ variations in the manipulated variables and in the measurable variables. These variations are due to sensor errors, analog-to-digital conversion errors, transmission errors, and noise. A deterioration model is used to add the effects of engine component deterioration over the useful life of the engine.

Figure 4 illustrates the principal steps in the control mode analysis process. A closed-loop control configuration is defined in terms of the number of closed loops to be used, the specific measurable variables to be used for closed-loop error feedbacks, and the engine-manipulated variables to be controlled closed loop. The linear engine model is then transformed to the selected mode. This process converts the selected measurable variables to matrix inputs and the corresponding closed-loop manipulated variables to matrix outputs. The transformed engine matrix is then used to calculate the overall performance parameter variations due to variations in the selected closed-loop measurable variables, the open-loop manipulated variables, and the engine component tolerances. Each element of the component and control tolerance models is assumed to be normally distributed and a root-sum-square process is used to calculate the overall performance parameter variations. These parameters are also assumed to be normally distributed. The deterioration model is then combined with the transformed engine matrix and used to calculate overall deterioration effects for each performance parameter. The deterioration model effects are assumed to be deterministic and a straight summation is used. Upper and lower 2-σ limits for each performance parameter are then obtained by combining the tolerance and deterioration effects.

The mode analysis procedure was used to examine the performance variations for potential closed-loop control configurations with 1, 2, 3, and 4 closed loops at each of the operating points along the selected VTH and HTV transition paths. Mode selection was based on the closed-loop control configuration, which resulted in the smallest variation in the more significant engine performance parameters (thrust, turbine temperature, stall margins, and rotor speeds). Table 2 summarizes the resulting control mode configurations selected by this process. Note that it involves a single closed-loop configuration for the idle region and four different four-loop configurations for the balance of the operating regime.

Table 3 contains the upper limits on turbine temperature and the lower limits on primary and remote thrust and fan

- **Select -** Variable Geometries $[M]$; Measurable Variables $[C]$; Performance Parameters $[P]$; Engine Tolerances & Decrements $[Q]$
- **Linear Engine Model** $\begin{bmatrix} C1 \\ C2 \\ P \end{bmatrix} = \left[\begin{array}{c|c} E & F \\ \hline G & H \end{array}\right] \cdot \begin{bmatrix} M1 \\ M2 \\ Q \end{bmatrix}$
- **Transform to Selected Mode** $\begin{bmatrix} M1 \\ C2 \\ P \end{bmatrix} = \left[\begin{array}{c|c} E' & F' \\ \hline G' & H' \end{array}\right] \cdot \begin{bmatrix} C1 \\ M2 \\ Q \end{bmatrix}$
- **Performance Tolerance** $P_{Ti} = \sqrt{\Sigma(G'_{ij}C_j)^2 + \Sigma(H'_{ij}M_{2j})^2 + \Sigma(H'_{ij}Q_{Tj})^2}$
- **Performance Deterioration** $P_{Di} = \Sigma H'_{ij} Q_{Dj}$
- **Lower and Upper Limits on Variations** $P_{Li} = P_{Di} - P_{Ti}$, $P_{Ui} = P_{Di} + P_{Ti}$

Fig. 4 Control mode analysis procedure.

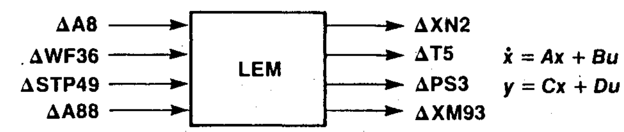

$$\begin{bmatrix} \Delta\dot{X}N2 \\ \Delta\dot{X}N25 \end{bmatrix} = \begin{bmatrix} a_{11} & a_{12} \\ a_{21} & a_{22} \end{bmatrix} \begin{bmatrix} \Delta XN2 \\ \Delta XN25 \end{bmatrix} + \begin{bmatrix} b_{11} & b_{12} & b_{13} & b_{14} \\ b_{21} & b_{22} & b_{23} & b_{24} \end{bmatrix} \begin{bmatrix} \Delta A8 \\ \Delta WF36 \\ \Delta STP49 \\ \Delta A88 \end{bmatrix}$$

$$\begin{bmatrix} \Delta XN2 \\ \Delta T5 \\ \Delta PS3 \\ \Delta XM93 \end{bmatrix} = \begin{bmatrix} 1 & 0 \\ c_{21} & c_{22} \\ c_{31} & c_{32} \\ c_{41} & c_{42} \end{bmatrix} \begin{bmatrix} \Delta XN2 \\ \Delta XN25 \end{bmatrix} + \begin{bmatrix} 0 & 0 & 0 & 0 \\ d_{21} & d_{22} & d_{23} & d_{24} \\ d_{31} & d_{32} & d_{33} & d_{34} \\ d_{41} & d_{42} & d_{43} & d_{44} \end{bmatrix} \begin{bmatrix} \Delta A8 \\ \Delta WF36 \\ \Delta STP49 \\ \Delta A88 \end{bmatrix}$$

Fig. 5 State-space linear engine model.

Table 2 Propulsion control modes

	RALS flow			Manipulated variables	
Control mode	Ratio, %	Closed loops	Sensed parameters	Closed loop	Open loop
Vertical	100	4	PCN2 T5 PS3 M93	A8 WF36 STP49 A88	STP22 WF6 WF86
Transition A	80-100	4	PCN2 T5 PS3 M93	A8 WF36 STP49 A88	STP22 WF6 WF86 A27
Transition B	0-80	4	PCN2 T5 PS3 M93	A8 WF36 STP49 STP22	A88 WF6 WF86 A80
Horizontal	0	4	PCN2 T5 PS3 M93	A8 WF36 STP49 STP22	WF6 A27
Idle	0	1	PCN2	WF36	A8 STP49 STP22 A27

Table 3 Typical performance variations

Operating point Mode	VTH transition Takeoff Vertical	80% RALS Transition B	MAX. Horizontal Horizontal	HTV transition FID Idle	60% RALS Transition B	80% RALS Transition A
%FG89(min)	−3.3	−5.7	—	—	−7.9	−4.0
%FG9 (min)	−6.9	−4.9	−4.3	−3.5	−2.6	−5.1
%SM2 (min)	−1.8	−1.8	−1.8	−1.9	−1.5	−1.8
%SM25 (min)	−2.1	−2.1	−2.1	−4.2	−10.0	−9.8
T41 (max) °F	47	48	43	82	23	31

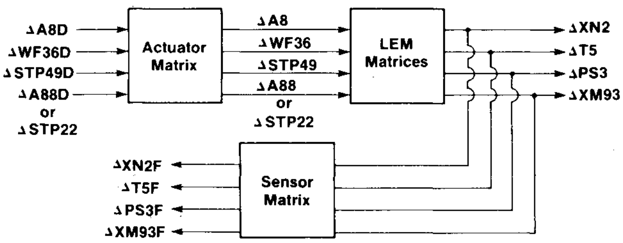

Fig. 6 Open-loop model.

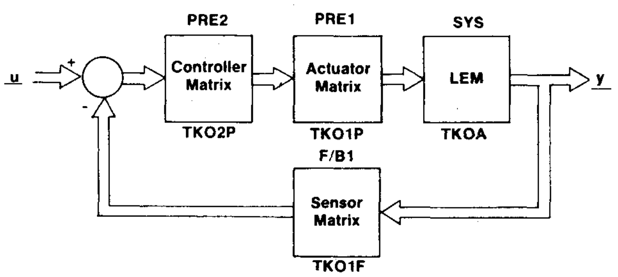

Fig. 7 K/Q matrix design technique.

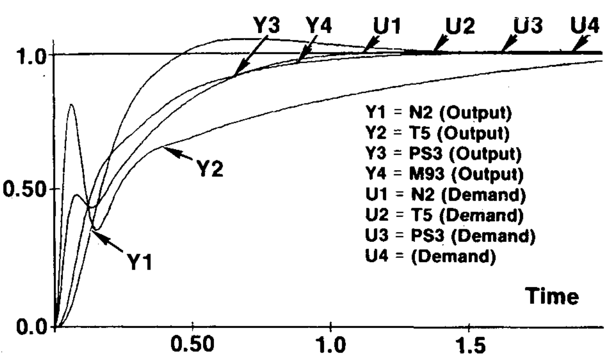

Fig. 8 Response to unit step demands at takeoff.

and compressor stall margin for the selected control configuration. These variations exceed normal experience for all thrust variations and for the stall margin variations at the high power range in the HTV regime. Potential techniques for reducing the thrust variations include the use of more direct thrust setting parameters, advanced sensor and sensor conditioning systems, and automatic compensation for individual engine tolerance and deterioration effects. The compressor stall margin loss might be accommodated by compressor discharge Mach number measurements, stator reset in the effected operating region, or by building additional stall margin into the compressor design. Additional investigations are required for addressing each problem.

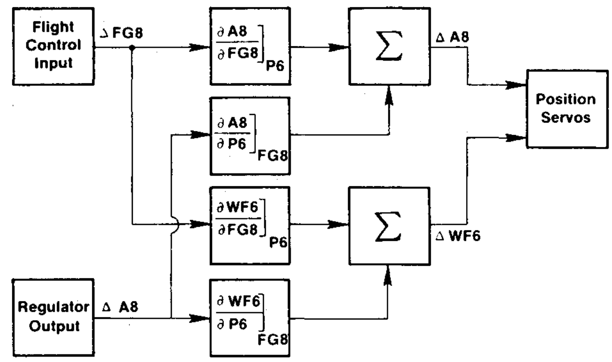

Fig. 9 ADEN feed-forward configuration.

Multivariable Regulator Design

Multivariable regulator designs were developed for each of the individual operating points along the VTH and HTV transition paths. The first step of the design process involved the development of transient linear engine models for each individual operating condition. These models include the effects of rotor dynamics and were obtained by running the steady-state cycle deck in an unbalanced torque mode. Figure 5 illustrates the state-space format used for each individual linear engine model. Nonlinear actuator models were developed to represent actuator dynamics and were approximated by linear transfer functions which were incorporated into a diagonal actuator matrix. Sensor dynamics were incorporated into a corresponding diagonal sensor matrix. Figure 6 illustrates the open-loop configuration used to combine the actuator and sensor matrices with the individual linear engine models.

Figure 7 illustrates the K/Q matrix design technique[4] which was used to develop a controller matrix for each individual operating condition in order to achieve quasidecoupling of the individual closed loops. A diagonal Q matrix was defined to represent the desired dynamic output of the closed-loop system. An iterative procedure was then used to develop a corresponding K matrix which could be used as the controller matrix to approximate the desired Q matrix output. Each resulting K matrix was expressed in Laplace transfer function form and contained proportional and integral gain coefficients for each of its elements:

$$K_{ij} = (a_{ij}S + b_{ij}) / S \tag{1}$$

Figure 8 contains a time-domain plot of the effects of simultaneous unit step demands to all four inputs of the closed-loop regulator at the takeoff condition along the VTH transition. These results are typical of similar studies performed at each of the other VTH and HTV operating conditions. In all cases, cross-coupling between the individual control loops was limited to the first quarter second and steady-state was achieved within 2 s.

Regulator gain schedules were then developed for each of the 16 proportional and 16 integral gain coefficients of the K matrix as a function of a derived flight control demand (FCD) parameter which represents position along the VTH or HTV transition paths. Separate schedules were determined to achieve the best linear regression fit for the major diagonal coefficients. Note that FCD is an implied function of thrust vector angle (TVA) and power lever angle (PLA), but no attempt has been made to define the functional relationship. A second series of time-domain plots of the effects of simultaneous unit step demands was generated using the resulting gain schedules. These results did not differ significantly from the earlier simulations based on the calculated gain schedules. The major effects of the regression errors were to increase the amount of loop interaction (high frequency) and to increase the time required to achieve steady-state conditions. The results were considered to demonstrate acceptable stability and response in all cases.

Feed-Forward System

The engine must provide thrust magnitude and direction corrections in response to flight control demands from the aircraft flight control system. Thrust magnitude corrections are provided by modulating the primary and remote augmentor fuel flows (WF6 and WF86) and their corresponding exhaust nozzle throat areas (A8 and A88). Thrust directional changes are provided by longitudinal deflection of the primary and remote nozzles and by transverse deflection of the remote nozzle. The current ADEN nozzle configuration does not have a transverse deflection capability.

The feed-forward system was designed to provide augmentor fuel flow and nozzle area schedules which could be used to respond to the thrust magnitude correction demands without effecting the engine rotor speeds, primary fuel flow, or the stall margin of the fan. This approach effectively decouples the flight control process from the engine regulation process and provides a rapid thrust response, which is not affected by the rotor inertias. Figure 9 illustrates the principle elements of the feed-forward system for the primary augmentor and ADEN. It uses a series of schedules derived from the linear engine model for:

1) The partial derivatives of A8 with respect to thrust at constant augmentor pressure, $(\partial A8/\partial FG8)]_{P6}$

2) The partial derivative of A8 with respect to augmentor pressure at constant thrust, $(\partial A8/\partial P6)]_{FG8}$

3) The partial derivative of WF6 with respect to thrust at constant pressure, $(\partial WF6/\partial FG8)]_{P6}$

4) The partial derivative of WF6 with respect to pressure at constant thrust, $(\partial WF6/\partial P6)]_{FG8}$

The fuel flow schedules are linear about the operating point and the area schedules include the nonlinear characteristics of the nozzle actuator. A similar feed-forward system is used for the remote augmentor and RALS nozzle.

The feed-forward system coordinates augmentor fuel flow and nozzle area corrections to produce small thrust changes at a fixed engine operating point and to produce small engine operating changes at fixed thrust. These capabilities were successfully demonstrated by hybrid computer simulations of the engine regulator and feed-forward system against a nonlinear transient model of the engine. A potential refinement of this concept would combine the individual primary and remote thrust corrections into an overall thrust correction error which would drive the regulator at a slower rate. This process would minimize migration from the center of the operating box of Fig. 2 in order to minimize the possibility of control saturation on subsequent correction commands. This refinement was not explored under the current program.

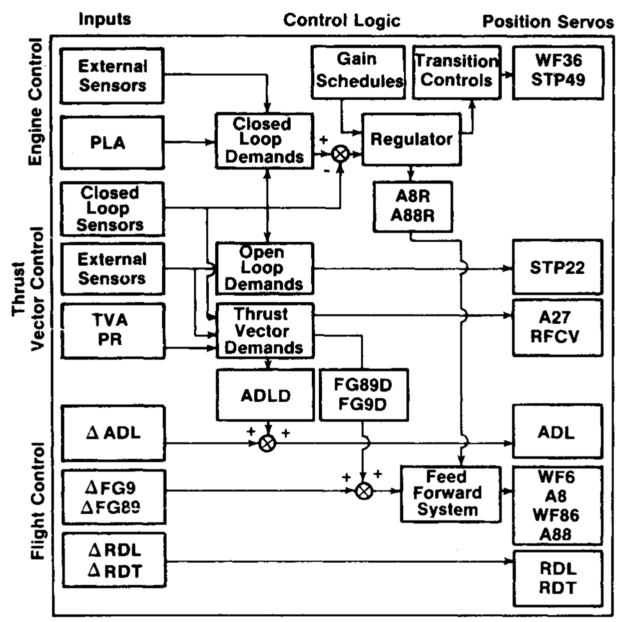

Fig. 10 Overall V/STOL control concept.

Overall Control Concept

Figure 10 contains a block diagram of an overall V/STOL propulsion control concept, which includes the multivariable regulator and feed-forward systems and which addresses requirements for engine control, thrust vector control, and flight control. It indicates control inputs, control outputs, and the principle interactions between the major control subsystems.

The engine control provides basic control functions such as the main fuel control, internal variable geometry control, speed regulation, and engine limit protection. Engine control inputs include external sensor data of environmental con-

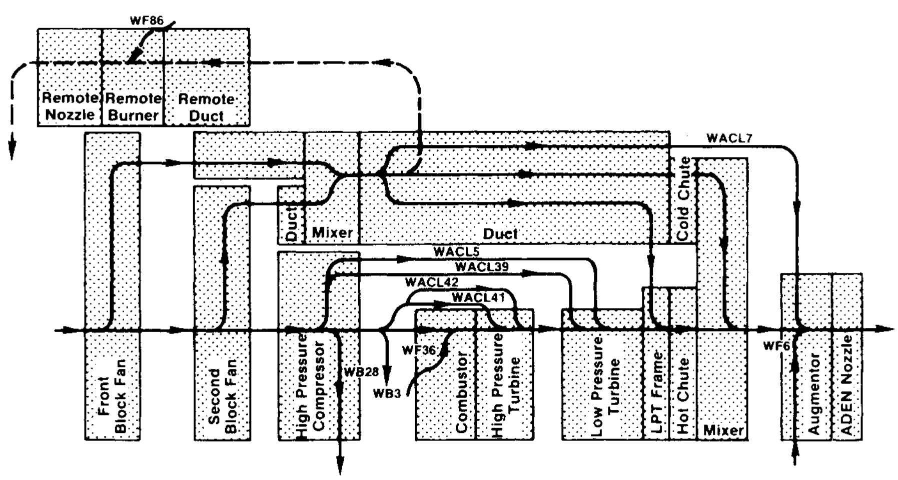

Fig. 11 Engine gas flow paths.

ditions, PLA demand, and closed-loop sensor data. The engine control logic includes:

1) closed-loop demand schedules for input to the multivariable regulator;

2) open-loop demand schedules for the open-loop manipulated variables;

3) gain schedules for establishing regulator proportional/integral gains as a function of PLA, TVA, and flight condition;

4) multivariable regulators which establish the demands for the closed-loop manipulated variables;

5) transition control for protecting the engine during large and/or fast throttle transients.

The transition controls include fuel acceleration and deceleration schedules for stall and blowout protection; engine speed, temperature, and pressure protection; and any special logic required for augmentor lightoff and shutdown protection.

The engine control logic provides output demands for primary fuel flow (WF36) and low-pressure turbine stator position (STP49) to the position sensors and nozzle area error demand signals (ΔA8R and ΔA88R) to the flight control system.

The thrust vector control sets the ADEN deflection angle and the nominal thrust split between the ADEN and RALS nozzle. Thrust vector control inputs include external sensor data, TVA demand, and a pitch rate (PR) or thrust ratio (TR) demand, which defines the ratio of the RALS to ADEN gross thrust requirement. The thrust vector control includes:

1) open-loop demand schedules for the rear VABI area (A27) and the remote flow control valve (RFCV), which set the flow split between the primary and remote augmentors;

2) the nominal ADEN deflection angle (ADL) which is set to the TVA demand;

3) RALS and ADEN nominal gross thrust demands (FG89D and FG9D). ADEN thrust demand is dependent upon PLA demand, flow split demand, and the external conditions. RALS thrust demand is determined from the ADEN thrust demand and the thrust ratio demands defined by TVA and PR. Note that the individual thrust demands set the nominal temperature in each augmentor.

The thrust vector control provides output demands for the VABI and RFCV to the position servos and nominal demands for the thrust magnitudes and ADEN deflection angle to the flight control system.

The flight control responds to individual ADEN and RALS thrust magnitude and deflection demands from the aircraft flight control system. It includes the following elements:

1) ADEN deflection demand (ΔADL) is added to the nominal demand signal from the thrust vector control (ADLD) to establish the total demand.

2) Thrust magnitude demands (ΔFG89 and ΔFG9) are added to the nominal demand signals from the thrust vector control to establish the total demands.

3) RALS deflection demands (ΔRDL and ΔRDT) are used to set the actual RALS deflections.

4) The nozzle area error signals from the engine control are input to the feed-forward system along with the actual thrust demands in order to set the augmentor fuel flow and nozzle area demands for the ADEN (WF6 and A8) and RALS (WF86 and A88) exhaust systems. Note that the feed-forward system modifies all four demand signals in order to trim nozzle area errors at constant thrust and to trim thrust corrections at constant engine operating point.

The flight control provides output demands directly to the corresponding position servos.

The current studies have defined the multivariable regulator, the regulator gain schedules, and the feed-forward system logic. Additional control logic and schedule design is necessary to complete the control system design process in order to provide propulsion system and control models for use in piloted aircraft-engine simulation programs. These studies include the development of: closed-loop and open-loop demand schedules, thrust vector control demand schedules, transition control schedules and control logic for engine limit protection, and feed-forward gain schedules.

Each of the above schedules must be examined along with the existing regulator gain schedules over their respective operating regimes to establish additional scheduling requirements with PLA, TVA, and external engine operating conditions. Control stability, response, and robustness must be examined at selected operating conditions to establish additional control logic or scheduling requirements for achieving acceptable operation over the total engine operating envelope.

Nonlinear Transient Engine Model

A simplified nonlinear transient model of the baseline engine was developed for use in the control design and development process and as a development tool in achieving a subsequent high-fidelity real-time capability for use in piloted simulations. A component level modeling approach was used and is shown in the engine gas flow path diagram contained in Fig. 11. The diagram shows the individual engine components modeled and the general sequence of calculations. Engine temperature, pressure, and flow calculations are performed at each of the indicated component interfaces. The component model is an approximation of the conventional aerothermo model used to establish engine steady-state and transient performance characteristics. Principle features of the simplified component model include:

1) Table lookup for thermodynamic properties and component performance maps were replaced by regression equations.

2) Component efficiency characteristics were absorbed into the component temperature and pressure ratio regressions.

3) Complex physical relationships for mixing, heat addition, and flow Mach numbers which involved exponentiation were replaced by polynomial regressions.

4) Rotor dynamics, mass conservation, and entropy conservation effects were retained and gasdynamic effects were omitted.

5) Heat storage effects were omitted from the initial model but must be added for the development of engine limit control schedules and logic.

Steady-state aerothermo models require an iterative solution for balancing internal flows and energies. This is accomplished by developing a partial derivative matrix from successive perturbations about an initial trial solution and the use of the matrix inverse for refining input estimates until an acceptable balance is achieved. Approximately 10-15 passes through the model are required to achieve an acceptable balance. Transient aerothermo models require a similar iterative solution but can continue to use the same partial derivative matrix for a number of successive transient time steps. This capability reduces computing requirements to the order of 1.5-2 passes through the model per time step. The simplified component-level model retains the aerothermo model iteration requirement but is restricted to a single pass per time step in order to minimize computation time for use in real-time simulation. This is accomplished by the use of a predetermined iteration matrix derived from the partial derivative matrices of a series of operating conditions.

The component-level model of the RALS/VCE engine represents about 190 lines of FORTRAN code and is about 30% larger than the real-time F404 component model contained in the full authority digital electronic control (FADEC) during recent engine tests.[5] Small throttle transients run on the RALS/VCE component model produced results which agreed with the more detailed transient aerothermo model within ±1% on most engine parameters. The component model has been used to develop linear models for the control mode studies and the regulator design process. It has also been used for evaluating transient characteristics of the engine and control system. The component model can be used as the basis for a high-fidelity real-time simulation capability for piloted simulation. Some refinements in the modeling approach may be necessary to achieve a simulation capability suitable for real-time piloted simulation.

Conclusions

V/STOL propulsion control requirements for an advanced supersonic V/STOL propulsion system can be met by integrating engine control, thrust vector control, and flight control subsystems. The regulator for the engine control subsystem can be derived from modern multivariable control design procedures, such as the frequency domain K/Q matrix design technique. Feed-forward logic and schedules can be used to integrate the engine, thrust vector, and flight control subsystems and to provide integrated control for the augmentor fuel flows and exhaust nozzle areas. The component-level modeling approach provides an effective balance between model fidelity and computer processing requirements for achieving a real-time simulation capability for use in piloted simulation programs.

Additional design and development efforts are, however, necessary to complete the V/STOL propulsion control design concept and to combine the control design with the engine model into a real-time simulation capability. These include the following:

1) Extension of the multivariable regulator and feed-forward gain schedules to cover the full operating range of the engine.

2) Development of full-range schedules for open-loop, closed-loop, and thrust vector control demands and for engine limit protection.

3) Further development and refinement of the component-level model to include heat storage effects for large transients, near-ground effects of distortion and re-ingestion, the full-range propulsion control model, and any modeling refinements necessary to preserve the real-time simulation capability.

Acknowledgments

The author is pleased to acknowledge the support of the NASA Lewis Research Center for the program described in this paper. Steady-state operating characteristics were developed by Dr. P.W. McDonald, control mode studies and regulator designs were developed by Dr. S.G. Day, and control logic and engine models were developed by Dr. R.C. Corley, all of the General Electric Aircraft Engine Business Group.

References

[1] Willis, W.S., "The Effects of Turbine Inlet Temperature and Engine Complexity on VCE/RALS Powered Supersonic V/STOL Aircraft," AIAA Paper 80-1853, Anaheim, Calif., Aug. 1980.

[2] Brown, R.H., "Integration of a Variable Cycle Engine Concept in a Supersonic Cruise Aircraft," AIAA Paper 78-1049, Las Vegas, Nev., July 1978.

[3] Lander, J.A., Nash, D.O., and Palcza, J.L., "Augmented Deflector Exhaust Nozzle (ADEN) Design for Future Fighters," AIAA Paper 75-1318, Anaheim, Calif., Sept. 1975.

[4] Edmunds, J.M., "Control System Design and Analysis Using Closed-Loop Nyquist and Bode Arrays," *International Journal of Control*, Vol. 30, No. 5, 1979, pp. 773-802.

[5] French, M.W., "Development of a Compact Real-Time Turbofan Engine Dynamic Model," SAE Paper 82-1401, Aerospace Congress and Exposition, Anaheim, Calif., Oct. 1982.